21. Khare, B. N. et al. in *Proc. First Int. Conf. Laboratory Research for Planetary Atmospheres* (NASA CP-3077) 327–339 (NASA, Washington DC, 1990).
22. Khare, B. N., Thompson, W. R., Sagan, C., Arakawa, E. T. & Lawn, J. J., *Bull. Am. astr. Soc.* **22,** 1033 (1990).
23. Strong, K. D. thesis, Univ. Oxford (1992).
24. Clark, R. N., Brown, R. H., Owensby, P. D. & Steele, A. *Icarus* **58,** 265–281 (1984).
25. Stevenson, D. J. in *Planetary Geology and Geophysics Abstracts* 65–66 (NASA, Washington DC, 1990).
26. Lunine, J. I. *Rev. Geophys.* (in the press).
27. Muhleman, D. O., Grossman, A. W., Butler, B. J. & Slade, M. A. *Science* **248,** 975–980 (1990).
28. Sagan, C. & Dermott, S. F. *Nature* **300,** 731–733 (1982).
29. Arvesen, J. C., Griffin, R. N. Jr & Pearson, B. D. Jr *Appl. Opt.* **8,** 2215–2232 (1969).

ACKNOWLEDGEMENTS. I thank C. McKay, R. Wagener, M. Lemmon, T. Owen and A. Grossman for discussion, and Y. Pendleton, K. Zahnle and W. Sharp for editorial comments. C.A.G. is an NAS/NRC resident research associate.

Radial deformation of carbon nanotubes by van der Waals forces

Rodney S. Ruoff, J. Tersoff*, Donald C. Lorents, Shekhar Subramoney† & Bryan Chan

Molecular Physics Laboratory, SRI International, Menlo Park, California 94025, USA
* IBM Thomas J. Watson Research Center, Yorktown Heights, New York 10598, USA
† Du Pont Co., Experimental Station, Wilmington, Delaware 19880-0228, USA

THE discovery of carbon nanotubes[1,2] has stimulated many theoretical studies of their physical properties[3–12], and their bulk synthesis[13] should soon make possible experimental measurements of these properties[14]. All studies so far have assumed that the nanotubes have perfect cylindrical symmetry. Here we show that van der Waals forces between adjacent nanotubes can deform them substantially, destroying this cylindrical symmetry. We present transmission electron microscopy images of two adjacent aligned tubes, about 100 Å in diameter, which show flattening of the tubes along the contact region. Calculations on two-layer nested nanotubes indicate that these deformations can be explained on the basis of van der Waals interactions. We predict that these effects should be observable at least for tubes as small as 20 Å in diameter, and suggest that they may have a significant influence on the tubes' physical properties.

The importance of the van der Waals interaction and its role in the energetics and elastic deformation of 'molecular' systems have been extensively discussed[15]. For example, the Lennard-Jones (L–J) 6–12 potential with appropriate parameters has been used to describe the van der Waals interaction between C atoms in fullerene solids such as C_{60}(s) and C_{70}(s), between C_{60} and graphite, and between planes of graphite. Empirical approaches that consist of summing over all unique C atom pairs have been essentially successful in their calculation of (low-pressure) properties of f.c.c. C_{60}(s), such as the lattice energy, zero-pressure bulk modulus, intermolecular separation, and bulk elastic properties[16–20]; the same can be said for calculation of the (low-pressure) cohesive energy, interplanar separation, zero-pressure bulk modulus, and elastic constants of graphite[21]. Using a similar approach, the binding energy between an isolated C_{60} molecule and a graphite plane has also been calculated and is surprisingly large, about 1 eV[22]. In these cases, the molecules or planes could be treated as rigid, and good agreement with experiment is obtained for a variety of properties even with this approximation. There are many other systems, however, in which large deformations in shape will occur, such as a liquid drop or a spherical vesicle, which each distort on a flat surface to become truncated spheres, or two adhering spherical vesicles[15]. Such 'molecular' systems are substantially larger, and more flexible, than C_{60}.

We performed transmission electron microscopy (TEM) of carbon growths that contain nanotubes, produced as described in ref. 13. In the TEM images we discovered two (nested) nanotubes that are almost perfectly aligned parallel to each other. These are shown in Fig. 1. One clearly sees sets of 10, 22 and 12 fringes. Thus the image represents two adjacent tubes, one of 10 nested layers and one of 12. The inner set of 22 fringes is strikingly more intense than the two sets of outer fringes. The diffraction conditions were such that small differences in interlayer (d) spacings, discussed further below, do not explain why the inner fringes are so much darker than the outer fringes. We can be sure Fig. 1 represents two adjacent tubes because the sum of outer fringes is equal to the number of inner fringes.

The two adjacent tubes A and B extend well beyond the section indicated in Fig. 1. There is a juncture where a 'loop' internal to tube A is apparent, having three layers (such internal loops appear in many nanotubes, and have been mentioned in the literature: see for example refs 1 and 2). At this juncture and beyond, the number of inner fringes increases to 25, and the number of outer fringes for the A tube increases to 13. Thus, the sum of outer fringes (13 + 12) is again equal to the sum of inner fringes, which confirms that we were viewing two adjacent nanotubes.

We propose that these large fringe intensity differences arise from a flattening of the nanotubes where they are pressed together by the van der Waals interaction. Further evidence of this is the compression of the interlayer spacings in the interface region. We have measured these directly from microphotometer scans of the high-resolution TEM negative. A typical scan perpendicular to the long axis of each tube is shown in Fig. 2. The intensity differences evident to the eye in Fig. 1 are quantitatively

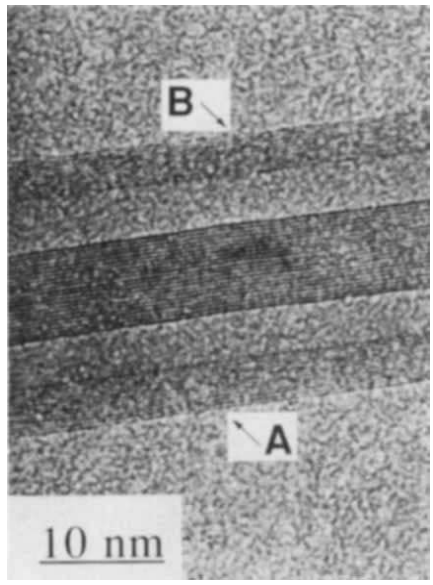

FIG. 1 High-resolution TEM micrograph of two (nested) adjacent nanotubes obtained at Scherzer defocus using a JEOL 2000FX TEM operated at 200 kV. Nanotube A contains 10 layers, and B contains 12 layers. The sum of the outer fringes is 22, which is equal to the sum of the inner fringes. Interlayer spacings are determined by calibrated microphotometry of the TEM negative, as described in detail in Fig. 2 legend and in the text. The outer diameter of A is 105 Å and the average interlayer spacing is 3.42 Å. The outer diameter of B is 116 Å and the average interlayer spacing is 3.47 Å. As is evident to the eye, the inner 22 fringes are more intense than the outer 10 and 12 fringes. About one third of the nanotube length from the actual negative is depicted in Fig. 1.

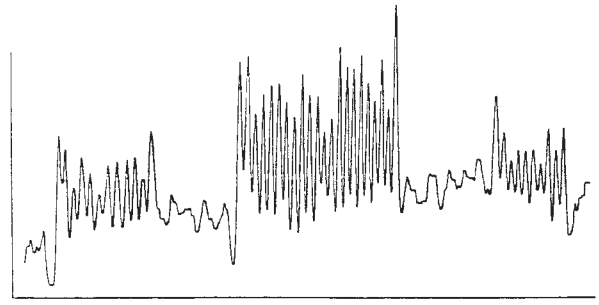

FIG. 2 Typical scan of fringe intensities of the TEM negative of the two adjacent (nested) nanotubes shown in Fig. 1. Although any one scan has fluctuations in peak intensities, it is clear that the inner fringes are substantially more intense than the outer fringes. The TEM negative is placed in a Jarrel–Ash scanning microphotometer which projects the image onto a slit. The fringes of the double tube are aligned parallel to the microphotometer slit and the negative is scanned and peak intensities recorded on a Linear Instruments chart recorder. The scan rate is 2.5 mm min^{-1}, the slit width is set to 43 microns, and the slit length to 1 mm; the plotted peak-to-peak distance is ~5.5 mm, and the average peak-to-peak distances are determined for tubes A and B by measuring the peak-to-peak separation across 8 peaks (tube A) and 10 peaks (tube B). The 2 outermost peaks are not included for each of A and B in determination of average interlayer (d) spacings. Distances are converted to Å units by calibration against distances obtained from TEM negatives of two standards: encapsulated α-LaC_2 crystals (ref. 25) and, separately, Au particles. The ultimate calibration is against powder X-ray diffraction of the α-LaC_2 particles (ref. 25). We determine the d spacing of the (2 0 0) planes of Au particles to be 2.03 Å with the α-LaC_2 standard; the actual value is 2.04 Å. Absolute distances reported in Table 1 are, therefore, good to 0.5%, and we expect relative distances to be good to 1 part in 500, which is the quoted accuracy of the translation stage of the microphotometer.

determined by the scanning microphotometer, as are the interlayer (d) separations.

As can be seen from Fig. 2, the peak heights obtained in a single microdensitometer scan are not uniform. Fluctuations in peak height for a particular layer are seen as a function of distance along the long axis of the tube. Also, one might expect the difference in average interlayer separations d_{inner} and d_{outer} to be better determined from several scans across the adjacent tubes. Three scans were obtained and average d values determined by two different methods. The distances obtained are summarized in Table 1, which clearly shows that the average d_{inner} is about 0.08 Å less than the average d_{outer}. Also, it is evident that there is a significant difference between the nested nanotubes A and B, as indicated by the absolute magnitudes of d_{inner} and d_{outer}. That is, it appears that the two nested nanotubes are fundamentally different in their geometry, which could be a result of different helicities. However, the deformation of each is quite similar, as reflected in the ($d_{outer} - d_{inner}$) values and peak height patterns obtained.

To compare with an isolated tube, we determined the two average d_{outer} values (each side) for a single (nested) nanotube, and found essentially no difference in the values for several scans. We also scanned the negative of the double tube in reverse order before scanning, and obtained results identical to those already discussed.

The data clearly show that the two nested nanotubes are deformed as a result of their contact. A direct view of this deformation would mean imaging the cross-section perpendicular to the long axis of the adjacent nanotubes of Fig. 1. Although we do not have such an image, we obtained understanding of the deformation from theoretical modelling.

We calculate the structure of a pair of nested carbon nanotubes, using a many-body interaction model for the intralayer forces[23], and an L-J model for the van der Waals interaction between atoms in different sheets, with L–J parameters fitted to graphite[21]. We average all van der Waals interactions in the direction parallel to the cylinder axis. Our nested tubes have an outer diameter of about 50 Å. (Nesting more than two tubes becomes numerically quite difficult.) The atom positions are relaxed until all forces are less than 0.004 eV $Å^{-1}$.

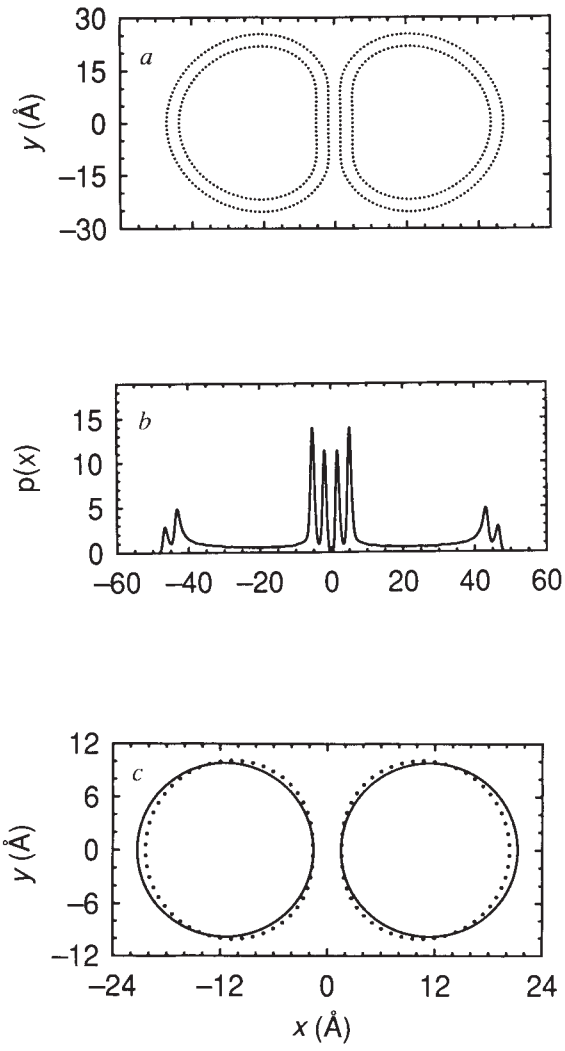

FIG. 3 *a*, Calculated deformation resulting from van der Waals forces between two (nested) nanotubes. Dots correspond to atom positions. The nanotube diameters are ~50 Å. Interlayer separations after deformation from the (nested) tube/(nested) tube van der Waals interaction are 3.44 Å (outer) and 3.39, 3.37, 3.39 Å (inner). *b*, Projected atom density from *a*. Note that the flattening evident in *a* is indicated by the larger projected atom density of the inner nanotube layers. *c*, Calculations for single-layer nanotubes 20 Å in diameter. The undeformed tubes are indicated by solid circles, and the relaxed tubes by dotted lines. The shift in the outer portion of the tubes is large enough (about 1.5 Å) to be observable experimentally.

TABLE 1 Nanotube average interlayer distances*

	A			B		
Scan	d_{outer}	d_{inner}	Δ	d_{outer}	d_{inner}	Δ
1	3.44	3.35	0.09	3.48	3.42	0.06
2	3.46	3.39	0.07	3.51	3.44	0.07
3	3.45	3.39	0.06	3.53	3.43	0.10
Average	3.45	3.38	0.07	3.51	3.43	0.08

Tube A has 10 nested nanotubes, tube B has 12; see Figs 1 and 2.
* All distances in Å. Distances obtained as described for Fig. 2.

Our individual tubes are generated by rolling a graphite sheet perpendicular to the 'a' axis, so the helical pitch is zero. Actually, the helicity is virtually irrelevant to the deformation. In the limit that the interlayer separation and tube radius of curvature are much larger than the intra-layer bond length, the tubes act as uniform elastic sheets. These sheets are isotropic in two dimensions because of the underlying hexagonal symmetry. Thus all of the properties discussed here are actually controlled by the planar-averaged van der Waals interaction, and the elastic constant for bending the graphite sheet, neither of which depends on helicity. Because the interlayer spacing is only a factor of 2.41 larger than the in-plane bondlength, small corrections could occur if two sheets had ordered stacking, like graphite. But this is not included in the calculation (because of our averaging of the interaction along the axis), and is unlikely to occur in reality (because sequential tubes may have different helicities, and so may not have graphite-like ordering; see ref. 24).

The resulting structure is shown in Fig. 3*a*. The deformation is evident: the nanotubes flatten where they are pressed together by the van der Waals interaction. This provides a compelling explanation for the contrast differences between the inner and outer layers of the high-resolution image shown in Fig. 1. The flattening of the inner planes leads to a locally thicker region of planes that satisfy the Bragg condition for diffraction. The resulting enhancement of contrast is illustrated in Fig. 3*b*.

As in the experiment, the calculation also shows a reduction in the interlayer spacing where the nanotubes are pressed together. Whereas the interlayer spacing at the far left and right of Fig. 3*a* is 3.44 Å, in the centre the respective spacings are 3.39, 3.37 and 3.39 Å. Thus the inner spacings are reduced by ~0.06 Å relative to the outer spacing, in good agreement with the experimental data in Table 1.

Nanotubes as small as 1 nm in diameter have been reported, and it is to be expected that the deformation will decrease with tube diameter. We have also performed calculations for single-layer tubes with smaller diameters, and find that measurable deformations remain at least for tubes as small as 20 Å in diameter (Fig. 3*c*). We have also investigated the influence of nesting by comparing the calculations for nested, two-layer tubes of 50- and 30-Å diameter with those for single-layer tubes. Nesting causes a moderate reduction in the extent of deformation.

We anticipate that van der Waals forces will be equally important in determining the structure of nanotubes bound to substrates, or into bundles, and that in all of these situations the intermolecular forces will play an important part in determining nanotube geometry and properties. Thus it seems unlikely that nanotubes are ever truly cylindrical. □

Received 13 April; accepted 17 June 1993.

1. Iijima, S. *Nature* **354,** 56–58 (1992).
2. Ajayan, P. M. & Iijima, S. *Nature* **358,** 23 (1992).
3. Iijima, S., Ichihashi, T. & Ando, Y. *Nature* **356,** 776–778 (1992).
4. Iijima, S., Ajayan, P. M. & Ichihashi, T. *Phys. Rev. Lett.* **69,** 3100–3103 (1992).
5. Saito, R., Fujita, M., Dresselhaus, G. & Dresselhaus, M. S. *Phys. Rev. B–Condensed Matter* **46,** 1804–1811 (1992).
6. Fujita, M., Saito, R., Dresselhaus, G. & Dresselhaus, M. S. *Phys. Rev. B–Condensed Matter* **45,** 13834–13836 (1992).
7. Dresselhaus, M. S., Dresselhaus, G. & Saito, R. *Phys. Rev. B–Condensed Matter* **45,** 6234–6242 (1992).
8. Jishi, R. A. & Dresselhaus, M. S. *Phys. Rev. B–Condensed Matter* **45,** 11305–11311 (1992).
9. Mintmire, J. W., Dunlap, B. I. & White, C. T. *Phys. Rev. Lett.* **68,** 631–634 (1992).
10. Mintmire, J. W. *et al. MRS Symp. Proc.* **247,** 339–343 (1992).
11. Sawada, S. I. & Hamada, N. *Solid State Commun.* **83,** 917–919 (1992).
12. Tersoff, J. *Phys. Rev.* B**46,** 15546–15549 (1992).
13. Ebbesen, T. W. & Ajayan, P. M. *Nature* **358,** 220–222 (1992).
14. Dresselhaus, M. S. *Nature* **358,** 195–196 (1992).
15. Isrealachvili, J. N. *Intermolecular and Surface Forces, with Applications to Colloidal and Biological Systems* 2nd edn. (Academic, London, 1991).
16. Girifalco, L. A. *J. phys. Chem.* **96,** 858–861 (1992).
17. Guo, Y. J., Karasawa, N. & Goddard, W. A. II *Nature* **351,** 464–467 (1991).
18. Cheng, A. L. & Klein, M. L. *J. phys. Chem.* **95,** 6750–6751 (1991).
19. Cheng, A. L. & Klein, M. L. *Phys. Rev. B–Condensed Matter* **45,** 1889–1895 (1992).
20. Sprik, M., Cheng, A. L. & Klein, M. L. *Phys. Rev. Lett.* **69,** 1660–1663 (1992).
21. Girifalco, L. A. & Ladd, R. A. *J. chem. Phys.* **25,** 693–697 (1956).
22. Ruoff, R. S. & Hickman, A. P. *J. phys. Chem.* **97,** 2494–2496 (1993).
23. Tersoff, J. *Phys. Rev. Lett.* **61,** 2879–2882 (1988).
24. Ge, M. & Sattler, K. *Science* **260,** 515–518 (1993).
25. Ruoff, R. S., Lorents, D. C., Chan, B., Malhotra, R. & Subramoney, S. *Science* **259,** 346–348 (1993).

ACKNOWLEDGEMENTS. Part of this work was conducted under the program 'Advanced Chemical Processing Technology,' which is consigned to the Advanced Chemical Processing Technology Research Association by the New Energy and Industrial Technology Development Organization and carried out under the Large-Scale Project administered by the Agency of Industrial Science and Technology, and Ministry of International Trade and Industry, Japan.

Synthesis of a tubular polymer from threaded cyclodextrins

Akira Harada*, Jun Li & Mikiharu Kamachi*

Department of Macromolecular Science, Faculty of Science, Osaka University, Toyonaka, Osaka 560, Japan

MUCH attention has been focused recently on the design and fabrication of large-scale molecular structures[1]. Carbon nanotubes formed by an arc-discharge method[2,3] have attracted particular attention. These tubes range from about 1 to 30 nanometres in diameter and a micrometre or so in length. To construct smaller tubes, direct chemical synthesis may be a more convenient approach. The cyclic oligomers of glucose known as cyclodextrins (CDs) would seem to be ideal candidates for the components of a molecular tube: they contain cylindrical cavities about 0.7 nm deep, with diameters of 0.45 nm, 0.7 nm and 0.85 nm for α-CD, β-CD and γ-CD respectively[4]. Lehn has recently reported the use of 'bouquet molecules' built from β-CD with long side chains as artificial ion channels[5]. We have previously prepared rotaxane supermolecules in which CDs are threaded on a polymer chain, and we[6] and others[7,8], have reported polyrotaxanes with many threaded CDs. Here we report the crosslinking of adjacent CD units in a polyrotaxane to create a molecular tube. By removing the bulky ends of the polymer thread, the tube can be unthreaded and can act as a host for reversible binding of small molecules.

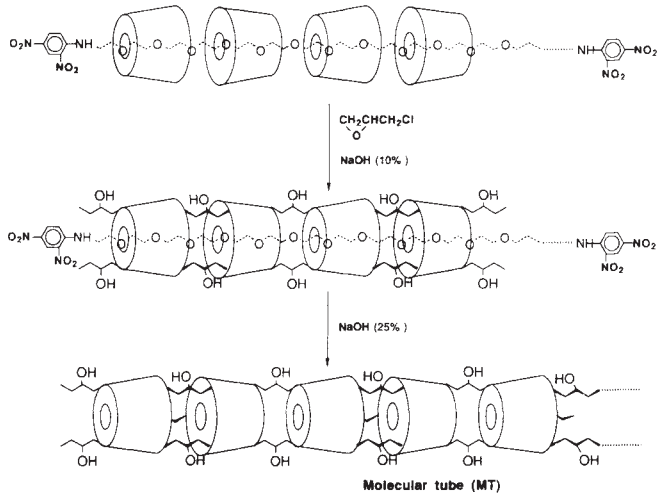

FIG. 1 Preparation of a molecular tube (MT) from polyrotaxane (MN).

Polyrotaxanes were prepared as described[6]. In this case poly (ethylene glycol) (PEG) of molecular mass 1,450 was used, because α-CD forms complexes with PEG of molecular weight 600–2,000 most efficiently. The complexes are nearly stoichio-

* To whom correspondence should be addressed.